Research Article

NMR IN BIOMEDICINE

Received: 25 January 2012, Revised: 10 May 2012, Accepted: 12 May 2012, Published online in Wiley Online Library: 2012

(wileyonlinelibrary.com) DOI: 10.1002/nbm.2827

A continuous-flow, high-throughput, high-pressure parahydrogen converter for hyperpolarization in a clinical setting

Jan-Bernd Hövener[a]*, Sébastien Bär[a], Jochen Leupold[a], Klaus Jenne[b], Dieter Leibfritz[a], Jürgen Hennig[a], Simon B. Duckett[c] and Dominik von Elverfeldt[a]

Pure parahydrogen (pH_2) is the prerequisite for optimal pH_2-based hyperpolarization experiments, promising approaches to access the hidden orders of magnitude of MR signals. pH_2 production on-site in medical research centers is vital for the proliferation of these technologies in the life sciences. However, previously suggested designs do not meet our requirements for safety or production performance (flow rate, pressure or enrichment). In this article, we present the safety concept, design and installation of a pH_2 converter, operated in a clinical setting. The apparatus produces a continuous flow of four standard liters per minute of ≈98% enriched pH_2 at a pressure maximum of 50 bar. The entire production cycle, including cleaning and cooling to 25 K, takes less than 5 h, only ≈45 min of which are required for actual pH_2 conversion. A fast and simple quantification procedure is described. The lifetimes of pH_2 in a glass vial and aluminum storage cylinder are measured to be T_{1C}(glass vial) = 822 ± 29 min and T_{1C}(Al cylinder) = 129 ± 36 days, thus providing sufficiently long storage intervals and allowing the application of pH_2 on demand. A dependence of line width on pH_2 enrichment is observed. As examples, ^{1}H hyperpolarization of pyridine and ^{13}C hyperpolarization of hydroxyethylpropionate are presented. Copyright © 2012 John Wiley & Sons, Ltd.

Keywords: parahydrogen; orthodeuterium; hyperpolarization; PASADENA; PHIP; SABRE

INTRODUCTION

The hyperpolarization of nuclear spins, such as ^{13}C, is a promising approach to access the hidden orders of magnitude of signals in MRI and MRS, holding great potential to improve medical diagnostics (1,2). Parahydrogen (pH_2)-based methods like SABRE (signal amplificatoin by reversible exchange) and PASADENA / PHIP (pH_2 and synthesis allow dramatically enhanced nuclear alignment / pH_2 induced polarization), employ the spin order inherent to pH_2 and critically rely on its purity (3–7,29). For maximum yield, an enrichment of ≈100% is required prior to any hyperpolarization experiment.

pH_2 is the spin-singlet isomer of dihydrogen, which has four spin states in total [one pH_2, three orthohydrogen (oH_2)] (Fig. 1). Following the Boltzmann distribution, these four states are approximately equally populated at room temperature (rtH_2), i.e. rtH_2 = 25% pH_2 and 75% oH_2. At lower temperatures, the equilibrium is shifted towards pH_2, reaching a pH_2 enrichment fraction (f_{pH2}) of ≈100% close to the boiling point of H_2 (20 K). Although the mechanism of interconversion between the two fractions is still under discussion (8,9), the lifetime of para-enriched hydrogen generally exceeds hours or days, dependent on its interactions with the storage container.

The spin properties of H_2 have been the subject of discussion since the early days of quantum mechanics (10–12). Several methods have been suggested for the production of pH_2 for various applications [e.g. refs. (13–15)]. All rely on contact with a catalyst at low temperatures [e.g. liquid N_2 at 77 K, f_{pH2}(77 K) ≈ 50%]. Recently, some experimental set-ups have been described aimed at the production of pH_2 for hyperpolarization (16,17). Generally, pH_2 production is not trivial. H_2 poses a considerable risk, being highly explosive when mixed with air at 4%-76%, and being an aggressive gas to some materials (hydrogen embrittlement). The previously described designs and procedures have a relatively low production rate (less than 1 standard liter per minute, L_s/min,

* *Correspondence to: Jan-Bernd Hövener, Medical Physics, Department of Radiology, University Medical Center Freiburg, Breisacher Straße 60A, 79106 Freiburg, Germany.*
E-mail: jan.hoevener@uniklinik-freiburg.de

a *J.-B. Hövener, S. Bär, J. Leupold, D. Leibfritz, J. Hennig, D. von Elverfeldt*
Medical Physics, Department of Radiology, University Medical Center Freiburg, Freiburg, Germany

b *K. Jenne*
Department of Occupational Safety, University Medical Center Freiburg, Freiburg, Germany

c *S.B. Duckett*
Department of Chemistry, University of York, Heslington, York, UK

Abbreviations used: *f_{oH2}, enrichment fraction of orthohydrogen; f_{pH2}, enrichment fraction of parahydrogen; FWHM, free width at half-maximum; L_s, standard liter; oH_2, orthohydrogen; PASADENA, parahydrogen and synthesis allow dramatically enhanced nuclear alignment; PHIP, parahydrogen induced polarization; pH_2, parahydrogen; P_c, cooling power; p_{max}, maximal pressure; QA, quality assurance; rtH_2, hydrogen at room temperature (≈75% oH_2 and 25% pH_2); SABRE, signal amplification by reversible exchange; T_{1C}, lifetime of pH_2–oH_2 conversion; $\rho(^1H)_{H2}$, density of hydrogen in dihydrogen gas; $\rho(^1H)_{water}$, density of hydrogen in water*

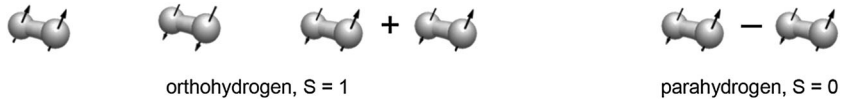

Figure 1. Spin isomers of dihydrogen: three ortho-spin states ($S = 1$, oH_2) and para-spin para or singlet state ($S = 0$, pH_2). Equally populated at room temperature, parahydrogen enrichment of the order of unity is achieved at low temperature, and pH_2 gas can be produced in large quantities. As a $S = 0$ spin particle, pH_2 does not give a NMR signal; all H_2 MR signals stem from oH_2.

SI units), low pressure (<10 bar), low enrichment (50%) or cannot be translated easily to a hospital setting. These may be the reasons why, to our knowledge, the implementation and operation of a production unit in a clinical setting have not yet been attempted.

Within the scope of the application of hyperpolarization to the life sciences, however, this is a prerequisite. Future applications are likely to be found in medical research, e.g. in hospitals, where the production of pH_2 is severely restricted. It is the aim of this contribution to resolve this problem, *en route* to routine hyperpolarization.

We have developed a high-throughput, high-pressure, continuous-flow pH_2 converter exceeding the specification of its predecessors. Furthermore, we present the safety concept, quality assurance (QA) and routine operation protocols with the goal to supply pH_2 safely for subsequent biomedical hyperpolarization research in medical institutions.

METHODS

Safety concept

The first step for the installation of a pH_2 unit is the development of a comprehensive safety concept and detailed risk assessment. Depending on the applicable laws, this will be guided by the hazards of H_2 as a pressurized ($p = 200$ bar) explosive gas, including the risk of ignition and hydrogen embrittlement (18,19). In agreement with the in-house safety department, the following requirements were developed.

(1) Construction of the conversion unit:

  (a) avoidance of an explosive H_2–air mix:

    (i) no bulk H_2 storage and no conversion indoors;
    (ii) strong ventilation of outside housing;

  (b) avoidance of spark sources:

    (i) no electronic components in the path of H_2;
    (ii) minimal electronics within the external housing;
    (iii) avoidance of temperatures above the flame point;
    (iv) avoidance of inductive spark sources;
    (v) avoidance of static charges;

  (c) avoidance of H_2 leaks:

    (i) overpressure relief valve;
    (ii) use of appropriate H_2-proof materials (e.g. embrittlement);

  (d) reduction of H_2 amount;
  (e) maximum safety in the case of an explosion:

    (i) immobilization of parts of external housing;
    (ii) pressure relief/explosion diaphragm for housing;

  (f) a pressure to store a sufficient amount of pH_2 (50 bar);
  (g) high throughput for short operational times;
  (h) a long lifetime of pH_2 (T_{1C}) within the storage cylinder to use the pH_2 produced for ≈1 week.

(2) Installation site:

  (a) H_2 supply: all H_2 outside within a protected compartment;
  (b) strong ventilation of outside housing;
  (c) no public access, distance to the public;
  (d) minimum transport of pH_2, short way to hyperpolarization and imaging site;
  (e) appropriate warning signs.

(3) Operation:

  (a) trained personnel only;
  (b) written manuals;
  (c) risk assessment;
  (d) regular QA checks for leaks, maintenance.

A QA protocol suitable for a clinical setting should address:

(1) equipment safety: materials, leaks, failure;
(2) personnel safety: training, manuals, documentation;
(3) high levels of pH_2 enrichment and fast (minutes) quantification thereof.

Ideally, existing and commercially available components should be employed.

For hyperpolarization experiments, we require:

(1) a para enrichment fraction close to 100%;
(2) a pressure of $pH_2 > 35$ bar.

Conversion unit and catalyst

A two-stage, closed-cycle helium cryocooler, cold head and catalyst chamber were ordered custom made to withstand an operational H_2 pressure of 50 bar (ARS-4HW and DE-204AE 9 K, radiation shield, vacuum shroud, ARS, Macungie, PA, USA; temperature controller SI 9700, Scientific Instruments, West Palm Beach, FL, USA; vacuum pump DS102, Varian, Palo Alto, CA, USA; all purchased from IDB, Duisburg, Germany). The helium compressor was connected to the in-house cooling water supply.

In this design, the catalyst was held in a cylindrical chamber instead of copper tubing, as applied previously [e.g. Malmø design (5,14), Fig. 2].

Several catalysts for oH_2–pH_2 conversion have been suggested (9,20–24). Using relatively coarse activated charcoal, close to unity para enrichment was achieved at flow rates of less than 1 L_s/min (rods of 3 mm in diameter and ≈5 mm in length, R3 Extra, Norit Deutschland GmbH, Riesbürg, Germany). The use of iron(III) oxide hydrate with a particle size of 300-500 μm (30-50 mesh, Molecular Products, Boulder, CO, USA) proved to be much more efficient [e.g. as suggested in ref. (24)].

NMR IN BIOMEDICINE

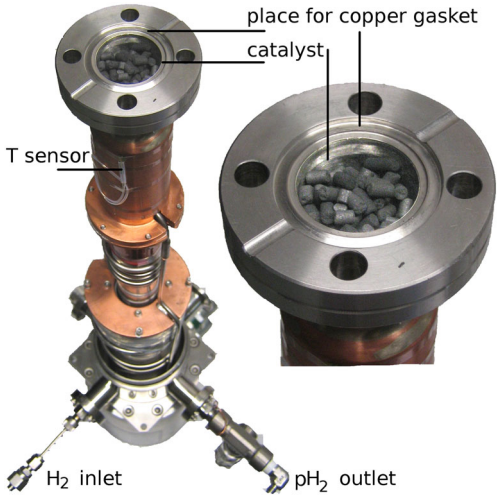

Figure 2. Photographs of a two-stage cryocooler with open catalyst chamber, filled with (rods of) activated charcoal, which was later replaced by iron(III) oxide (hydrate) of smaller mesh size (≈300-500 μm), which enabled higher production rates.

Previous studies on the conversion of liquid H_2 have shown that smaller iron hydroxide particles (<150-600 μm) do not improve the yield further (25).

Considering the ortho-deuterium production described by Gamliel *et al*. (17), we assume that the set-up is suited for ortho-deuterium conversion, although we did not verify this experimentally. When used as a spin-order source in a hydrogenation reaction, deuterium may provide a prolonged hyperpolarization lifetime.

For adjustment of the H_2 flow, a needle valve and an oxygen flow meter were used (converted to values for hydrogen, Karl Heck GmbH, Rüdesheim, Germany). An aluminum bottle equipped with a three-way valve (stainless steel, Swagelok) and an optional pressure regulator was employed as storage container. With a weight of 2 kg and a volume of 5 L, the cylinder is easily transportable from the conversion unit to the hyperpolarization laboratory, where it was stored in a gas safety cabinet. Other parts, e.g. the housing of the set-up, were constructed by an in-house machine shop; the gas lines (copper and stainless steel) were mounted by a specialized local company.

MR methods

A small-bore 7-T MRI system (Biospec 70/20, Bruker BioSpin MRI GmbH, Ettlingen, Germany), equipped with a quadrature mouse coil, was employed (inner diameter, 3.9 cm; active length, 8 cm; Rapid Biomedical GmbH, Rimpar, Germany). Unlocalized ^{1}H spectra (TR = 200 ms, 256 averages) were acquired of the empty coil (to determine the origin of the background) and glass vials filled with H_2 or N_2 (99.999%, Sauerstoffwerk Friedrichshafen, Friedrichshafen, Germany). The glass vials (borosilicate 3.3; V = 100 mL; inner diameter, 3 cm; Rotilabo, Carl Roth GmbH & Co. KG, Karlsruhe, Germany) were sealed with a turn-over flange stopper (type 407030–5, Compagnie de Saint Gobain, Aachen, Germany), extending the active region of the coil by approximately 5 cm. The vial was held in place using a holder made from hydrogen-free polytetrafluoroethylene to insure reproducible positioning (custom made). The samples were taken by guiding the respective gas from the storage cylinder through a flexible hose and syringe needle, penetrating the septum sealing the glass vial. Another needle released the gas from the vial. A slow flow was chosen to ensure reproducible filling of the vial at ambient pressure. Neither the needle nor the optional pressure regulator in the path of pH_2 affected the enrichment.

Because of the low rtH_2 signal, the local field homogeneity was optimized using the signal of a water-filled vial of the same dimensions and position. Using the automated iterative adjustment of the first-order shims (provided by the manufacturer), the water resonance exhibited a free width at half-maximum (FWHM) of 50 Hz after nonlocalized excitation. When second-order shims were added, the FWHM was reduced to ≈20 Hz

The acquired data were processed using the manufacturer's software (paravision 5.1). A numeric computing environment (MATLAB R2011B, The Mathworks, Natick, MA, USA) was used to fit a Lorentzian function to the isolated H_2 resonance [providing the line width and area = peak height × (FWHM/2) × π]. The same software was used to fit a monoexponential decay to the time course of the signal intensities obtained by monitoring the pH_2 to rtH_2 conversion (Fig. 5A).

The reproducibility of f_{pH2} was evaluated by filling a vial alternately with N_2, rtH_2 and pH_2 five times. After each filling, the vial was placed into the magnet and ^{1}H MRS data were acquired. By subtracting the signal of the N_2-filled vial (background), the oH_2 signal was isolated for subsequent quantification.

RESULTS

Performance

Guided by the specified requirements, we constructed a set-up allowing the production of $f_{pH2} \approx 98\%$ at a maximum pressure of p = 50 bar and a rate of ≥4 L_s/min at a temperature set to T_{set} = 25 K (Fig. 4). The 'critical interval', at which substantial amounts of pH_2 flow through the system, was less than 1 h for the production of up to 250 L_s of pH_2 compressed to 50 bar (Table 1). As this amount of pH_2 was stable and sufficient for a couple of days of experiments, the production cycle needed to be repeated less frequently, adding to the overall safety.

The full production cycle included a relatively long N_2 flush of the gas lines, catalyst chamber and storage cylinders to remove air and potential impurities, and a consequent H_2 flush to remove N_2, which would freeze whilst cooling. In total, less than 5 h were required for start-up, production and shut-down.

Safety

To comply with the safety concept, the unit was separated into two parts: The electronic devices were placed inside a maintenance building in the attic of the institute, and all H_2-containing parts, including the cold head and bulk H_2 bottles, were installed on the outside. Connections were fed through a wall of approximately 30 cm and sealed (Fig. 3).

The protective housing was mounted to the outside wall of the building. Joints allow its roof to open to guide the pressure of a potential deflagration or explosion upwards, away from any operator, reducing the risk of demolishing the housing and injury.

Table 1. Procedure of parahydrogen (pH_2) production. Steps in which significant amounts of H_2 are present in the system are indicated in bold italic type. It should be noted that, at no time, may H_2 be filled in a storage cylinder containing air

Step number	Duration (min)	Step	Operation
1	55	Flushing the converter (including catalyst chamber) with N_2	R2, V2, V4 open
2	***5***	***Flushing the converter (including catalyst chamber) with H_2***	***R1, V3, V2, V4 open***
3	180	Evacuation of vacuum shroud, start cooling	V1 open
4	***3 × 1***	***pH_2 production: flushing the storage cylinder with pH_2***	***R1, V2, V3, V5, V6 open***
5	***45***	***pH_2 production: filling of storage cylinder with pH_2***	***R1, V2, V3, V5, V6 open***
	288	Total time of production cycle	
	53	***Total time whilst H_2 is within the set-up***	

R, pressure regulator; V, valve.

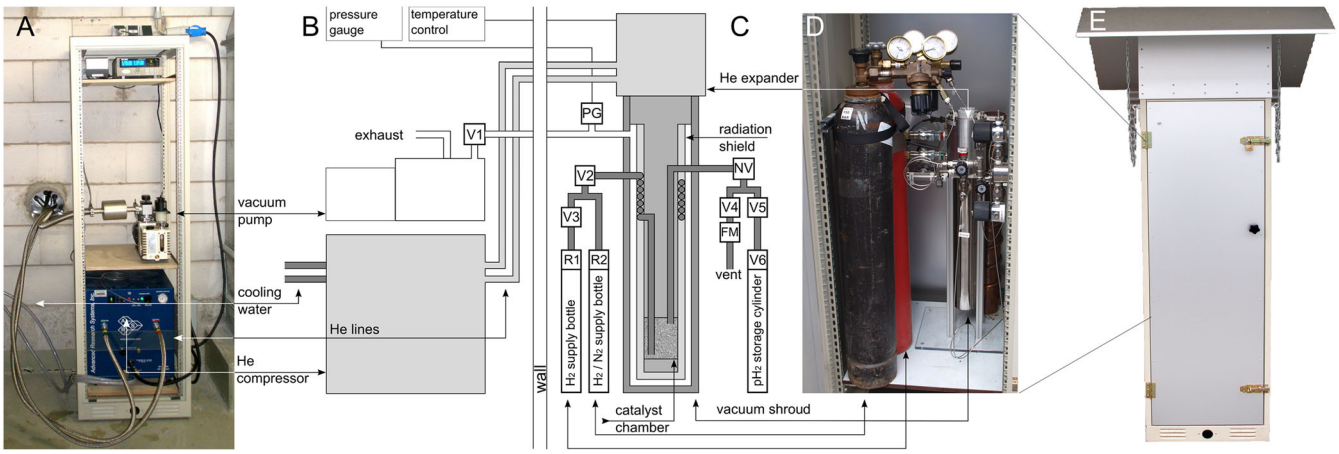

Figure 3. Photographs and schematic view of the parahydrogen (pH_2) production unit: (A) helium compressor, vacuum pump, temperature and pressure control; (B, C) schematic representation; (D) H_2, N_2 supply bottles, cold head; (E) external housing. To comply with safety, the electronics (A, B) and H_2-containing parts (C–E) were separately installed on the inside and outside of a maintenance building on the roof of the institute, respectively. FM, flow meter; (N)V, (needle) valve; PG, pressure gauge; R, pressure regulator.

In addition, all walls of the compartments were connected to one another by chains. In total, the required footprint was less than 3 m^2.

This concept does not make the production safe by definition. The overall safety, however, was increased with respect to the regulations imposed by law and the hospital's internal safety board.

Quantification and QA

To quantify the pH_2 enrichment fraction, MRS was chosen, as all NMR spectrometers and clinical MR systems with a spectroscopy option are suitable. The measurement of MR-invisible pH_2, however, is not straightforward since (a) the signal of gas is very low because of the low spin density at ambient pressure [$\rho(^1H)_{H2} \approx 1/22$ mol/L, $\rho(^1H)_{water} \approx 110$ mol/L], (b) the resonance of a gas is much broader than a liquid and (c) only oH_2 gives rise to a MR signal.

For example, at a realistic enrichment of 99%, only 1% (oH_2) of the sparse gas gives rise to a broad MR signal. As a result, the H_2 signal was well below the background induced by other protons. We found the housing of the transmit–receive coil to be the source of the background signal observed (Fig. 4, red spectra). The H_2 signal was isolated by subtracting the background signal of an N_2-filled vial from the signal of a vial filled with pH_2 (Fig. 4).

To quantify the signal of a sample of unknown enrichment, a reference of known pH_2/oH_2 fraction was needed. A straightforward choice is to wait until the pH_2-enriched sample has reached room temperature equilibrium (rtH_2, a mix of 75% oH_2 and 25% pH_2). However, this experiment may take a long time, and hydrogen may leak out. To avoid scan times of multiple hours, we quantified the pH_2 enrichment fraction with respect to a second sample of rtH_2 from bulk storage obtained and scanned promptly after the pH_2 sample. The enrichment fraction f_{pH2} was calculated from the signals of both [Equation [1], e.g. in ref. (17)]:

$$\begin{aligned} f_{pH2} &= 1 - \left(3S_{pH2}\right)/\left(4S_{rtH2}\right) \\ f_{oH2} &= 1 - f_{pH2} \end{aligned} \qquad [1]$$

Routinely, $f_{pH2} \approx 98\%$ was achieved. Its quantification takes about 13 min (Table 2). The coefficient of variance was measured to be $c_v(rtH_2) = 4\%$ for the rtH_2 signal and $c_v(pH_2) = 22\%$ for the residual signal in pH_2 samples (each $n = 5$). This amounts to an absolute error of the enrichment fraction of $\Delta f_{pH2} = 0.02$ (using Gaussian error propagation).

While monitoring the pH_2 to oH_2 conversion, we observed a change in the line width of the oH_2 resonance (Fig. 5b). For $f_{pH2} \approx 80\%$ to 25%, the line width decreased from ≈1400 Hz to 1075 Hz. A similar finding has been reported previously (17).

Lifetime of pH_2

The conversion of highly para-enriched H_2 gas (e.g. $f_{pH2} = 98\%$) to room temperature equilibrium ($f_{pH2} = 25\%$) was examined when stored in a glass vial or aluminum cylinder. The glass vial was placed

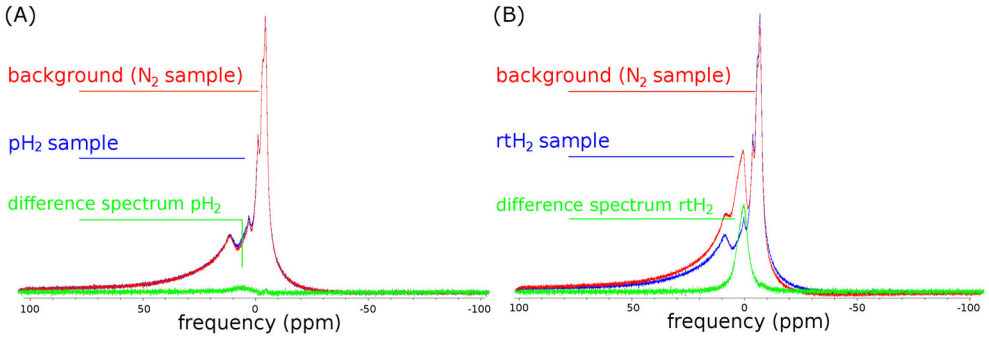

Figure 4. Quantification of the parahydrogen (pH_2) enrichment fraction. ^{1}H MR spectra of glass vials filled with N_2 (red, background), pH_2 (blue, left) and room temperature H_2 (rtH_2, blue, right). By subtraction of the background (red), the signals of both samples were isolated (green, S_{pH2}, S_{rtH2}), allowing the quantification of the pH_2 enrichment: $f_{pH2} = 1 - 0.75\ S_{pH2}/S_{rtH2} = 98\%$ (pulse-acquire sequence; number of averages, 256; TR = 200 ms; $B_0 = 7$ T). The background signal originates from the materials of the housing of the transmit–receive coil.

Table 2. Protocol for the quantification procedure of parahydrogen (pH_2) enrichment using MRS, carried out prior to hyperpolarization experiments. The actual scan time required is indicated in bold italic type

Duration	Step
4 min	***Preparation of MR scanner (shim, adjustments)***
3 min	Filling of vial with pH_2
3 min	Filling of vial with rtH_2
60 s	***Placement of pH_2 sample, acquisition of spectrum***
60 s	***Placement of rtH_2 sample, acquisition of spectrum***
60 s	***Placement of N_2-filled sample, acquisition of spectrum***
13 min	Approximate total time for quantification
7 min	***Total scan time required***

rtH_2, room temperature H_2.

in the MRI system for the entire observation time. Samples from the aluminum storage cylinder were taken on different days. A monoexponential decay function was fitted to the time course of the signal intensities. The relaxation constant for pH_2-oH_2 conversion (T_{1C}) in the glass vial with the rubber septum, $T_{1C} = 822 \pm 29$ min, corresponds well to the values reported elsewhere [$T_{1C} = 846 \pm 5$ min (16), Fig. 5). The lifetime in the storage cylinder was rather long, estimated to $T_{1C} \approx 120$ days. This exceeds the requirements for the pH_2 lifetime, being defined by the use of a pH_2 batch for 1 week (the purity will only be reduced by ≈5%).

Hyperpolarization

To demonstrate the use of pH_2 for hyperpolarization, proton signal amplification was achieved by employing the reversible exchange technique SABRE (26–28), [Fig. 6A, B]. The method of pH_2 synthesis allowed dramatically enhanced nuclear alignment of ^{13}C-hydroxyethylpropionate using a spin-order transfer sequence [PASADENA] (3,6,14,29–31), Fig. 6C, D].

DISCUSSION

Performance

A high-throughput, continuous-flow pH_2 converter was designed specifically for hyperpolarization in a clinical setting. Implications to safety were considered. As a result, we obtained a unit that exceeds the flow and pressure achieved by previously described systems (13,16,17) without sacrificing safety demands. Indeed, the flow rate of at least 4 L$_s$/min enables the 'interval-at-risk' (during which H_2 flows through the set-up) to be kept short. Compared with lower pressure systems, the high pressure (routinely 35 bar; maximum 50 bar) allows the storage of an increased pH_2 amount per bottle, reducing the repetitions of the production cycle

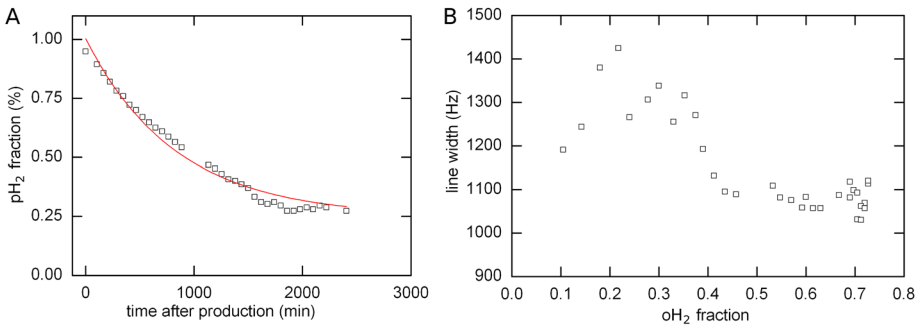

Figure 5. Parahydrogen (pH_2) fraction (f_{pH2}, Equation [1]) monitored with ^{1}H MRS during thermal equilibration to room temperature H_2 (rtH_2) in a glass vial at 7 T (A), and ^{1}H line width of the same data as a function of the orthohydrogen (oH_2) fraction (B). When subjected to a monoexponential fit, a relaxation constant of T_{1C}(pH_2, glass vial) = 822 ± 29 min was obtained ($R^2 = 0.98$, reduced $\chi^2 = 10^{-3}$). Because of the low signal intensity, the line width of the first two data points in (B) was not reliable. The mean line width for $oH_2 > 70\%$ was 1075 ± 35 Hz ($n = 11$).

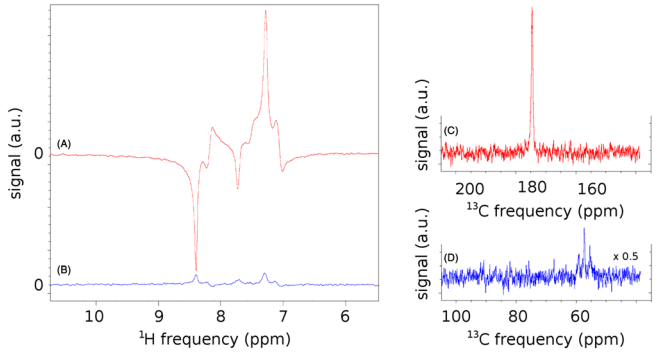

Figure 6. Hyperpolarization using parahydrogen. ^{1}H MR spectra of pyridine (≈1.5 M) in $^2H_4$-methanol, hyperpolarized using SABRE (signal amplification by reversible exchange) (A, red) and in thermal equilibrium (B, blue, $B_0 = 7$ T, $n = 1$). ^{13}C spectra of hyperpolarized 1-^{13}C,2,3-$^2H_3$-hydroxyethylpropionate (C) and 70% ethanol at thermal equilibrium (D). It should be noted that (C) was acquired with one acquisition only at a concentration of ^{13}C of 2 mM, whereas $n = 8$ acquisitions were required to record (D) at a concentration of ^{13}C of 131 mM.

(higher flow rates are likely, but were not used). These specifications exceed our current needs, as hyperpolarization experiments aimed for biomedical applications are usually conducted at a maximum of 10 bar [PASADENA (14,31)] or ambient pressure [SABRE (27)]. However, $p_{max} = 50$ bar provides some reserves for future experiments which may require higher pressures, e.g. for the hydrogenation reaction.

What is the limit of the pH_2 production rate? In practice, it is constrained by two factors: the contact time of pH_2 and the catalyst, and the power of the set-up to cool and discard the heat of H_2.

At the cost of a potentially shorter contact time, we decided against the usual catalyst-filled tubing, and instead mounted a cylindrical container on the second stage of the cryostat to facilitate changing of the catalyst (Fig. 2). No internal substructure of the chamber is installed at present, although it may further increase the contact time and production rate, as suggested elsewhere (16).

To estimate the limits imposed by the cryocooler, we compared its cooling power (P_c) with the energy ΔE required to bring H_2 from ≈300 K to 25 K (ΔT). A rough estimate of the energy required may be obtained by considering H_2 to be a diatomic ideal or van der Waals' gas:

$$\Delta E = \left[\frac{5\, N\, k_B\, \Delta T}{2}\right] \qquad [2]$$

where k_B is Boltzmann's constant, N is the amount of molecules and ΔT is the temperature difference.

There are two stages in the cryocooler: the first provides $P_c = 18$ W at 77 K; the second provides $P_c = 8$ W at 20 K.

In the first stage, assuming all H_2 is cooled from 300 to 77 K ($\Delta T = 223$ K), 4635 J are required for 1 mol, giving a maximum flow rate of $flow_{1st} = 5{,}2$ L$_s$/min for $P_c = 18$ W. In the second stage, to cool the gas further from 77 to 25 K, $E = 1080$ J/mol are required. At $P_c = 9$ W, this corresponds to a flow rate of $flow_{2nd} = 11{,}2$ L$_s$/min. Thus, the power at the first stage limits the process. This assessment may differ from reality, but provides a rough estimate for the maximum flow rate that can be realized at a given cooling power (note, however, that the heat capacity of the catalyst has not been taken into account).

Safety

Separation of the apparatus, keeping the main H_2 reservoir outside the building, allowed us to meet the major safety requirements. This is different to previously described set-ups (e.g. 30,32). Spark sources were avoided as, apart from the commercial cryocooler and vacuum pump, no electronics, such as electromagnetic valves, were employed, and none were present along the transportation route of H_2. In addition to greater safety, we expect increased robustness with this approach. We refrained from evacuating the storage cylinders prior to refilling in order to avoid exposing the (hot) vacuum pump to H_2. Instead, when the storage cylinder was used for the first time, air was removed by thoroughly flushing with N_2 prior to pH_2 filling. In routine operation, the bottle contains pH_2 at a pressure of 9–10 bar before it was refilled, preventing air from entering.

Generally, to exclude the risk of an explosion, we avoided any contact of H_2 with air in closed systems by thoroughly flushing with an inert gas and using intact seals and appropriate rules of conduction.

H_2 (and even D_2) may be supplied in small quantities by hydrolysis or chemical reaction, reducing the risk and extent of an explosion (17). However, we require a relatively high pH_2 pressure, which these methods do not provide at a reasonable cost. We chose to employ H_2 in $V = 10$ L standard steel cylinders pressurized to 200 bar, which are readily available at high purity (i.e. H_2 '5.0', 99.999%).

Apart from initial issues with the catalyst chamber and insulating vacuum (which were corrected by the manufacturer), there have been no incidents, leaks or failures reported so far (the system has been running for more than 6 months). The safety procedures do not impose unreasonable requests in the routine production of pH_2.

Although these measures ensure overall safety and allow operation in a hospital, we emphasize that the apparatus does not meet the standards of a governmentally approved, clinically safe medical product, e.g. for patient use. Safety regulation at other sites will vary.

Quality assurance

The pH_2 fraction is controlled currently on a weekly basis prior to hyperpolarization experiments. As no drop in performance has been recorded so far, this interval may be prolonged. The choice of a quantification method was guided by practicability. Although other relatively simple methods were suggested (33–36), we decided on an MR-based method for the quantification of pH_2 enrichment, as all groups interested in hyperpolarization have access to some (N)MR systems. A previous publication on QA (30) focused on the hyperpolarization experiment rather than on the production of pH_2, with only little information on pH_2 QA being given. Quantification by NMR has been used by some groups previously (16,17,32).

A recently suggested method of monitoring the full para to ortho conversion provides high accuracy but is of limited use for routine applications (16). Although this method is elegant and has virtue in requiring only one sample (which is measured immediately after production for several days to monitor the equilibration process), generally, a continuous scan time of multiple hours is not feasible on a routine basis. The conversion time may be shortened by introducing a relaxation agent. With only 3×60 s, the actual acquisition time of the quantification

protocol employed here was very short. In total, including the preparation and filling of the two vials with pH_2 and rtH_2, about 13 min were required for the entire quantification procedure (Table 2). A further reduction of the scan time by 50% was achieved when the scanner was prepared after the filling of the samples. This increases the time that pH_2 resides in the vial by a few minutes. As the relaxation was slow ($T_{1C} = 822 \pm 29$ min), however, it can be neglected and does not compromise the quantification. In taking two samples, an additional error was introduced, as it was difficult to assess whether both samples were filled to the exact same amount. However, there was no concern of H_2 leaking from the vial over a time of 50 h, and the absolute error of f_{pH2} was low ($\Delta f_{pH2} = 0.02$). We found that shorter TRs decreased the quality of the background subtraction, which may be attributed to incomplete relaxation at short TRs. At TR = 200 ms and 256 acquisitions, the scan time was still very short, and sufficient reproducibility was provided. In total, we achieved a reproducibility which was sufficient for our purpose of monitoring the pH_2 production efficiency.

It should be noted that the major source of error was the stability of the scanner and subtraction routine of the background signal, as small drifts, e.g. in temperature or frequency, deteriorate the result (no temperature control was installed in the tomograph). Rapid consecutive acquisitions help to reduce this effect. The background was found to originate from the coil. Indeed, we were able to image the coil's housing in another study using zero TE (ZTE) sequences (37). The use of proton-free materials, as suggested for ZTE imaging, may overcome this. NMR spectrometers lacking heavy coil encasings do not face this problem (16,17,32).

As the quantification procedure was reduced to a fraction of 1 h, we consider the effort of taking and scanning two samples worthwhile.

Lifetime and line width of H_2

We found that the time constant for the pH_2–oH_2 conversion in the glass vial, $T_{1C} = 822 \pm 29$ min (Fig. 5A), corresponds well to the values found by Feng *et al.* (16) ($T_{1C} = 846 \pm 5$ min). The relaxation of pH_2 in the storage cylinder ($T_{1C} \approx 120$ days), however, was twice as long as reported (16) ($T_{1C} = 63.7 \pm 8.3$ days). This difference may be attributed to different materials of the storage cylinders. A future step may be the integration of a non-MR-based quantification device into the conversion unit, e.g. based on thermal conductivity (13,34).

We found the line width to be dependent on the pH_2 fraction (Fig. 5B). For $f_{pH2} \approx 80\%$ to 25%, the line width decreased from 1400 Hz to 1075 Hz. Gamliel *et al.* (17) reported a line width for $f_{pH2} = 50\%$ of ≈840 Hz, and ≈630 Hz for rtH_2, using a high-resolution, 500-MHz NMR spectrometer.

Although the relationship of the longitudinal relaxation time T_1 to the oH_2–pH_2 content has been studied in detail (38,39), little information was available about the line width. Purcell *et al.* (40) reported a constant line width for H_2 gas at pressures between 10 and 30 bar in a small volume of ≈0.8 cm^3 at 0.68 T, presumably at room temperature, using continuous-wave MR. Two counteracting mechanisms were suggested to explain this observation: line narrowing with increasing pressure as a result of more effective averaging of the residual local field fluctuations, and a thermal relaxation increasing the line width proportional to the pressure. These results may be compared with our findings when the oH_2 fraction was interpreted as the partial oH_2 pressure [$p(oH_2)$]. The pressure range, however, was very different, but the findings are not in conflict. We observe an increased line width at very low, close to zero, $p(oH_2)$, which was approaching a constant value at $p(oH_2) \approx 0.75$ bar [≈1075 Hz here and 629 Hz in ref. (17)]. Purcell *et al.* (40) reported a constant line width of ≈1060 Hz between 10 and 30 bar.

Differences in MR systems and samples may be the reason why the line width reported by Gamliel *et al.* (17) was smaller by ≈40% (in particular with respect to the field homogeneity of an 11.8-T, high-resolution spectrometer with NMR tubes compared with a 7-T animal imager with large test tubes). Another reason may be the glass vials employed. These were made of 3.3 borosilicate glass (which is used for NMR tubes). A T_2* effect of the material seemed unlikely, but was hard to exclude. Coating of the inner walls of the tube may help to reduce this potentially line-broadening mechanism.

This is only a first step *en route* to routine *in vivo* hyperpolarization. Similar concepts of safety and QA are required for subsequent parts of the hyperpolarization experiment, polarizer and chemistry (e.g. removal of the hydrogenation catalyst).

CONCLUSION

A high-throughput, high-pressure pH_2 production unit was presented, which meets the safety regulations for use in a clinical setting. pH_2 enrichment of ≈98 ± 2% was achieved regularly at a rate of 4 L_s/min and a pressure maximum of 50 bar. A reproducible and fast quantification procedure is presented, and a dependence of the line width on the pH_2 fraction is observed. When stored in an aluminum cylinder, a lifetime of the order of 100 days allowed conversion to short-lived hyperpolarization on demand.

Acknowledgements

Part of this work was supported by the Innovationsfonds Baden-Württemberg and the Academy of Excellence of the German Science Foundation.

REFERENCES

1 Bhattacharya P, Chekmenev EY, Perman WH, Harris KC, Lin AP, Norton VA, Tan CT, Ross BD, Weitekamp DP. Towards hyperpolarized ^{13}C-succinate imaging of brain cancer. J. Magn. Reson. 2007; 186: 108–113.
2 Roth M, Koch A, Kindervater P, Bargon J, Spiess HW, Munnemann K. (13)C hyperpolarization of a barbituric acid derivative via parahydrogen induced polarization. J. Magn. Reson. 2010; 204(1): 50–55.
3 Bowers CR, Weitekamp DP. Para-hydrogen and synthesis allow dramatically enhanced nuclear alignment. J. Am. Chem. Soc. 1987; 109 (18): 5541–5542.
4 Chekmenev EY, Hövener J-B, Norton VA, Harris KC, Batchelder LS, Bhattacharya P, Ross BD, Weitekamp DP. PASADENA hyperpolarization of succinic acid for MRI and NMR spectroscopy. J. Am. Chem. Soc. 2008; 130: 4212–4213.
5 Golman K, Axelsson O, Johannesson H, Mansson S, Olofsson C, Petersson JS. Parahydrogen-induced polarization in imaging: subsecond C-13 angiography. Magn. Reson. Med. 2001; 46(1): 1–5.
6 Bowers CR, Weitekamp DP. Transformation of symmetrization order to nuclear-spin magnetization by chemical-reaction and nuclear-magnetic-resonance. Phys. Rev. Lett. 1986; 57(21): 2645–2648.
7 Duckett SB, Newell CL, Eisenberg R. More than inept – parahydrogen and inept + give unprecedented resonance enhancement to C-13 by direct H-1 polarization transfer. J. Am. Chem. Soc. 1993; 115(3): 1156–1157.

8 Buntkowsky G, Walaszek B, Adamczyk A, Xu Y, Limbach HH, Chaudret B. Mechanism of nuclear spin initiated para-H-2 to ortho-H-2 conversion. Phys. Chem. Chem. Phys. 2006; 8(16): 1929–1935.
9 Wigner E. Concerning the paramagnetic conversion of para-ortho hydrogen. III. Z. Phys. Chem. Abt. B 1933; 23(1/2): 28–32.
10 Heisenberg W. The quantum theory of line structure and the anomalous Zeeman effect. Z. Phys. 1921; 8: 273–297.
11 Born M, Heisenberg W. The quantum theory of molecules. Ann. Phys. 1924; 74(9): 1–31.
12 Bonhoeffer KF, Harteck P. Characteristics of parahydrogen. Z. Elektrochem. Angew. Phys. Chem. 1929; 35: 621–623.
13 Tam S, Fajardo ME. Ortho/para hydrogen converter for rapid deposition matrix isolation spectroscopy. Rev. Sci. Instrum. 1999; 70(4): 1926–1932.
14 Hövener J-B, Chekmenev EY, Norton VA, Weitekamp R, Harris KC, Perman WH, Robertson L, Weitekamp DP, Ross BD, Bhattacharya P. PASADENA hyperpolarization of ^{13}C biomolecules: equipment design and installation. Magn. Reson. Mater. Biol. Phys. Med. 2009; 22(2): 111–121.
15 Tom B, Bhasker S, Miyamoto Y, Momose T, McCall B. Producing and quantifying enriched para-H2. Rev. Sci. Instrum. 2009; 80(016108): DOI: 10.1063/1.3072881.
16 Feng B, Coffey A, Colon R, Chekmenev EY, Waddell K. A pulsed injection parahydrogen generator and techniques for quantifying enrichment. J. Magn. Reson. 2012; 214: 258–262.
17 Gamliel A, Allouche-Arnon H, Nalbandian R, Barzilay C, Gomori J, Katz-Bull R. An apparatus for production of isotopically and spin-enriched hydrogen for induced polarization studies. Appl. Magn. Reson. 2010; 39(4): 329–345.
18 Safety Standard for Hydrogen and Hydrogen Systems. NASA, Office of Safety and Mission Assurance: Washington DC; 1997.
19 Beeson H, Woods S. Guide for Hydrogen Hazards Analysis on Components and Systems. NASA, Johnson Space Center: Houston, TX; 2003, TP-WSTF-937.
20 Farkas A. The thermal parahydrogen conversion. Z. Phys. Chem. Abt. B 1930; 10(6): 419–433.
21 Farkas L, Sachsse H. Concerning the homogenic catalysis – the para–ortho hydrogen conversion under the influence of paramagnetic ions. II. Z. Phys. Chem. Abt. B 1933; 23(1/2): 19–27.
22 Farkas L, Sachsse H. Concerning the homogenic catalysis – the para–ortho hydrogen conversion under the influence of paramagnetic molecules. I. Z. Phys. Chem. Abt. B 1933; 23(1/2): 1–18.
23 Eley DD, Rideal EK. The catalysis of the parahydrogen conversion by tungsten. Proc. R. Soc. London Ser. A 1941; 178(A975): 0429–0451.
24 Svadlenak RE, Scott AB. The conversion of ortho-hydrogen to parahydrogen on iron oxide–zinc oxide catalysts. J. Am. Chem. Soc. 1957; 79 (20): 5385–5388.
25 Weitzel DH, Park OE. Iron catalyst for production of liquid para hydrogen. Rev. Sci. Instrum. 1956; 27: 57–58.
26 Adams R, Aguilar J, Atkinson K, Cowley M, Elliot P, Duckett S, Green G, Khazal I, Lopez-Serrano J, Williamson D. Reversible interactions with para-hydrogen enhance NMR sensitivity by polarization transfer. Science 2009; 5922: 1708–1711.
27 Adams R, Duckett S, Green R, Williamson D, Green G. A theoretical basis for spontaneous polarization transfer in non-hydrogenative parahydrogen-induced polarization. J. Chem. Phys. 2009; 131(194505): DOI: 10.1063/1.3254386.
28 Atkinson K, Cowley M, Duckett S, Elliot P, Green G, Lopez-Serrano J, Khazal I, Whitwood A. Para-hydrogen induced polarization without incorporation of para-hydrogen into the analyte. Inorg. Chem. 2009; 48: 663–670.
29 Natterer J, Bargon J. Parahydrogen induced polarization. Prog. Nucl. Magn. Reson. Spectrosc. 1997; 31: 293–315.
30 Hövener J-B, Chekmenev EY, Norton VA, Harris KC, Perman WH, Weitekamp DP, Ross BD, Bhattacharya P. Quality assurance of PASADENA hyperpolarization for ^{13}C biomolecules. Magn. Reson. Mater. Biol. Phys. Med. 2009; 22(2): 123–134.
31 Goldman M, Johannesson H. Conversion of a proton pair para order into C-13 polarization by rf irradiation, for use in MRI. C. R. Phys. 2005; 6(4–5): 575–581.
32 Bhattacharya P, Harris K, Lin AP, Mansson M, Norton VA, Perman WH, Weitekamp DP, Ross BD. Ultra-fast three dimensional imaging of hyperpolarized C-13 in vivo. Magn. Reson. Mater. Biol. Phys. Med. 2005; 18(5): 245–256.
33 Bradshaw TW, Norris JOW. Observations on the use of a thermal conductivity cell to measure the para hydrogen concentration in a mixture of para and ortho hydrogen gas. Rev. Sci. Instrum. 1987; 58(83): 83–85.
34 Eucken A, Hiller K. The detection of the conversion of orthohydrogen into parahydrogen by means of measurement of the specific heat. Z. Phys. Chem. Abt. B. 1929; 4(1/2): 142–157.
35 Grilly ER. A simple thermal conductivity analyzer for ortho-para hydrogen. Rev. Sci. Instrum. 1952; 24(72): 72–73.
36 Weitzel DH, White LE. Continuous analysis of orthoparahydrogen mixtures. Rev. Sci. Instrum. 1955; 26(290): 290–292.
37 Hövener J-B, Zwick S, Leupold J, Eisenbeiβ A-K, Eisenbeiβ A-K, Scheifele C, Schellenberger F, Hennig J, Elverfeldt D, Ludwig U. Dental MRI: Imaging of soft and solid components without ionizing radiation. *Journal of Magnetic Resonance Imaging* Article first published online: 15 Jun 2012; DOI: 10.1002/jmri.23712.
38 Abragam A. Principles of Nuclear Magnetism. Oxford University Press: London, New York, Toronto; 1985.
39 Bloom M. Nuclear spin relaxation in hydrogen: I. The gas. Physica 1957; 23(1–5): 237–247.
40 Purcell EM, Pound RV, Bloembergen N. Nuclear magnetic resonance absorption in hydrogen gas. Phys. Rev. 1946; 70: 986–987.